Biochimica et Biophysica Acta 1788 (2009) 676–685

Contents lists available at ScienceDirect

Biochimica et Biophysica Acta

journal homepage: www.elsevier.com/locate/bbamem

Transport of glutathione transferase-fold structured proteins into living cells

Melanie J. Morris, Scott J. Craig, Theresa M. Sutherland, Philip G. Board, Marco G. Casarotto *

The John Curtin School of Medical Research, Australian National University, Canberra, A.C.T., 0200, Australia

ARTICLE INFO

Article history:
Received 4 September 2008
Received in revised form 21 October 2008
Accepted 27 October 2008
Available online 6 November 2008

Keywords:
Glutathione transferase
Endocytosis
Protein structure
Protein transduction domain

ABSTRACT

Glutathione transferases are a family of enzymes that are traditionally known to contribute to the phase II class of detoxification reactions. However, a novel property of the *Schistosoma japonicum* glutathione transferase (Sj.GST26) involves its translocation from the external medium into a variety of different cell types. Here we explore the efficiency and mechanism of cell entry for this class of protein. Using flow cytometry and confocal microscopy, we have examined the internalisation of Sj.GST26 into live cells under a variety of conditions designed to shed light on the mode of cellular uptake. Our results show that Sj.GST26 can effectively enter cells through an energy-dependent event involving endocytosis. More specifically, Sj.GST26 was found to colocalise with transferrin within the cell indicating that the endocytosis process involves clathrin-coated pits. A comprehensive study into the cellular internalisation of proteins from other classes within the GST structural superfamily has also been conducted. These experiments suggest that the 'GST-fold' structural motif influences cellular uptake, which presents a novel glimpse into an unknown aspect of GST function.

© 2008 Elsevier B.V. All rights reserved.

1. Introduction

The cellular membrane performs the dual role of allowing selective passage of specific biological molecules into the cell, whilst simultaneously acting as a formidable barrier that blocks the free exchange of molecules between the cytoplasm and extracellular environment. The fundamental structure of membranes is the phospholipid bilayer, into which various proteins, glycolipids and cholesterol are inserted. A vast array of molecules have the ability to cross the cellular membrane either by diffusion processes or by protein-mediated mechanisms that involve transport proteins and ion channels. Such molecules are responsible not only for cell maintenance and function, but in some cases also have the ability to trigger cell death [1]. Intriguingly, it has been reported in a qualitative study that a glutathione transferase (GST) from *Schistosoma japonicum* (Sj.GST26) can be internalised from the medium into a variety of mammalian cell types [2,3].

GSTs are a family of enzymes that are generally considered to contribute to the phase II class of detoxification reactions. In this role they conjugate the tripeptide glutathione (GSH) to a wide range of electrophilic and generally hydrophobic compounds that may be of endogenous or exogenous origin. Whilst there are reports of GSTs interacting with cell membranes [4,5], so far there has been no physiological role identified for a complete extra- to intracellular translocation of exogenous cytosolic GSTs. Therefore it is unclear whether the observed translocation of Sj.GST26 is an isolated, non-specific event, or indeed whether this family of enzymes could represent a novel class of proteins capable of efficiently entering cells.

Despite the relatively low sequence homology between classes, all cytosolic GSTs share the same general structure — an N-terminal thioredoxin fold motif and a strongly helical C-terminal domain as shown in Fig. 1. Together this structure has been termed the 'GST-fold'. In the current study we have quantitatively investigated the entry of Sj.GST26 into cells through a series of experiments that consider the efficiency, mechanism and specificity associated with cellular uptake. In light of our results, we expanded the scope of this research to consider different classes of mammalian cytosolic GSTs, as well as other proteins that possess a GST structural fold but do not exhibit any known GST enzyme activity. Furthermore, the effect of mutating key, active-site residues related to GST enzyme function was examined with respect to cell entry. Our results show that Sj.GST26 enters cells with an efficiency comparable to the receptor-mediated transferrin ligand, and that the mechanism of cell entry involves endocytosis. We find that the ability of Sj.GST26 to enter cells extends not only to other GST enzymes, but also to molecules

Abbreviations: PTD, protein transduction domain; GST, glutathione transferase; GSH, glutathione; GSH-S, glutathione synthetase; CLIC2, chloride intracellular channel 2; GDAP1, ganglioside-induced differentiation-associated protein 1; Grx2, glutaredoxin-2; BSA, bovine serum albumin; GFP, green fluorescent protein; PBS, phosphate-buffered saline; FACS, fluorescence-activated cell sorting; OG, Oregon Green; TRITC, tetramethylrhodamine isothiocyanate; 7-AAD, 7-amino-actinomycin D; ER, endoplasmic reticulum; Sj.GST26, *Schistosoma japonicum* GST; TCEP, tris-(2-carboxyethyl) phosphine; PNRC, perinuclear recycling compartment; CME, clathrin-mediated endocytosis; Tfn, transferrin

* Corresponding author. The John Curtin School of Medical Research, GPO Box 334, Canberra City, A.C.T. 2601, Australia. Tel.: +61 2 61252598; fax: +61 2 61250415.
E-mail address: marco.casarotto@anu.edu.au (M.G. Casarotto).

0005-2736/$ – see front matter © 2008 Elsevier B.V. All rights reserved.
doi:10.1016/j.bbamem.2008.10.018

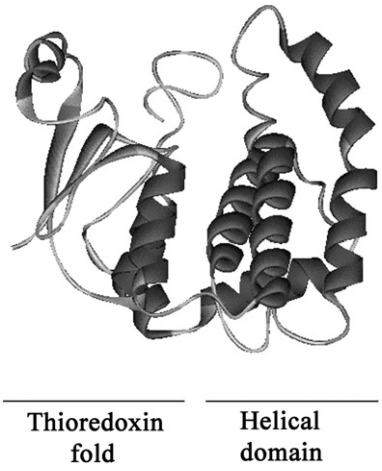

Fig. 1. Structural GST-fold. Ribbon diagram demonstrating the GST-fold structure of Sj. GST26 complexed to glutathione sulfonic acid. Note the N-terminal thioredoxin fold and C-terminal α-helices. The figure was generated by the use of the DS modelling 1.1 program (Accelrys) from the accession bank file RCSB_1M99.

that possess a GST-fold structure, and conclude that cell translocation is independent of GST enzyme function.

2. Materials and methods

2.1. Materials

Bovine serum albumin and all cellular inhibitors were purchased from Sigma, with the exception of sodium azide (Ajax Chemicals). Neutral dextran-TexasRed (70 kDa), ER-Tracker™Red, BODIPY TR C_5-ceramide, human transferrin solution, Oregon Green 488 carboxylic acid succinimidyl ester '5-isomer' and Alexa Fluor 633 carboxylic acid succinimidyl ester were from Molecular Probes. Human transferrin-TRITC was from Jomar Diagnostics. 7-amino-actinomycin D (7-AAD) was from BD PharMingen.

2.2. Expression and labelling of recombinant proteins

All proteins used in this study with the exception of transferrin and BSA, were expressed in *E. coli* and purified by affinity chromatography. GSTA1-1, GSTM2-2, GSTP1-1 and the *S. japonicum* GST (Sj.GST26) were purified by glutathione agarose affinity chromatography as previously described [6–9]. Other GSTs (GSTO1-1, GSTZ1-1), GST-fold proteins (CLIC2, GDAP1), and glutathione synthetase (GSH-S) which do not bind to glutathione agarose were expressed with poly-His tags and purified by nickel sepharose affinity chromatography as described previously [10–14]. Plasmids encoding the GST-fold proteins Ure2 from *S. cerevisiae*, and Glutaredoxin-2 (Grx2) from *E. coli*, were constructed from amplified genomic DNA cloned into the pDEST17 vector (Invitrogen) using the Gateway cloning technology (Invitrogen). Poly-His tagged proteins were expressed overnight at 30 °C using 1 mM IPTG and purified by nickel sepharose affinity chromatography as described previously [15].

GST mutations were performed using the QuickChange site-directed mutagenesis kit (Stratagene) and verified by DNA sequencing.

Purified proteins were dialysed into PBS prior to fluorescent labelling of primary aliphatic amines with Oregon Green succinimidyl ester according to the manufacturer's instruction. Labelled proteins were passed through size-exclusion sephadex columns then dialysed for 48 h against PBS at 4 °C to ensure efficient removal of free dye. Protein concentration and fluorophore to protein ratios were calculated from protein absorbance at 280 nm and 496 nm according to the manufacturer's labelling protocol. Commercial bovine serum albumin and human transferrin were reconstituted in PBS and labelled with Oregon Green in the same manner. All Oregon Green-labelled proteins were aliquoted and stored at −20 °C.

The cycle3 green fluorescent protein (cyc3GFP) and mOrange constructs were amplified from pDEST47 (Invitrogen) and pRSETB-mOrange [16] respectively, and inserted into the Sj.GST26 expression plasmid pDEST15 (Invitrogen) using the Gateway cloning method (Invitrogen). Sj.GST26-cyc3GFP and Sj.GST26-mOrange fusion proteins were expressed from pDEST15-GFP and pDEST15-mOrange transformed BL21(DE3) cells overnight at 30 °C using 1 mM IPTG, and purified by glutathione agarose affinity chromatography as described previously [9]. The eluted proteins were dialysed overnight at 4 °C against PBS and concentrated using ultrafiltration. The purified Sj.GST26-mOrange protein was thiol-labelled with Oregon Green 488 maleimide in the presence of TCEP, according to the manufacturer's instruction. Thiol rather than amine-labelling was performed to preferentially label only the GST portion of the fusion protein (the mOrange protein contains no cysteines). Unreacted fluorophore was removed by dialysis overnight against PBS at 4 °C. A standard curve of green/orange fluorescence was constructed using protein diluted in PBS adjusted to pH 4.5, 5.0, 5.5, 6.0, 6.5 and 7.0 using dual channel fluorescence measured by fluorescence spectroscopy.

2.3. Cell culture

Cell lines were obtained from ATCC and routinely maintained in RPMI 1640 medium, supplemented with 10% fetal bovine serum (FBS) (v/v), 2 mM glutamine and 2 g/L $NaHCO_3$ at 5% CO_2 and 37 °C. Cultures were passaged using PBS containing 0.05% trypsin and 0.02% EDTA (v/v). All cell culture reagents were purchased from Gibco.

2.4. Flow cytometry

To quantitatively investigate the cellular uptake of all GST-fold proteins, as well as the effect of various inhibitors upon this process, L-929 cells were seeded at a density of 8×10^4 per well in 12-well plates (Nunclon) in 10% FBS/RPMI 1640 medium. The next day cells were rinsed with serum-free RPMI 1640 medium before addition of inhibitors or fluorescently-labelled proteins in serum-free medium. Following protein incubation, cells were washed several times with PBS and detached by trypsinization for 10 min at 37 °C. Cells were centrifuged at 4 °C, washed in cold PBS containing 2% FBS (v/v) then resuspended in 2% FBS/PBS containing 0.5 μg/mL 7-amino-actinomycin D (7-AAD). Cells were incubated at room temperature in the dark for 10 min prior to fluorescence-activated cell sorting of 10^4 counts on a FACScan flow cytometer (Becton Dickinson). Cells with 7-AAD fluorescence were considered nonviable and excluded from histogram acquisition. The geometric mean fluorescence of the viable population was divided by the fluorophore to protein ratio (calculated according to labelling protocol — see method above) and this standardised value considered representative of the amount of intracellular protein.

2.5. Quantification of GST uptake

To compare the rate of uptake of various GST-fold proteins, and BSA and GSH-S controls, the Oregon Green-labelled proteins were added to cells in serum-free media at 200 nM concentration in a time course over 3 h, and cells incubated at 37 °C/5% CO_2. Untreated cells were used for the initial zero time point. Samples were harvested and prepared for flow cytometry simultaneously as described above. The geometric mean fluorescence of viable cells in each incubation time point was standardised to the fluorophore to protein ratio for that particular protein, as mentioned previously. In this manner the intracellular fluorescence of different proteins could be quantitatively compared over time.

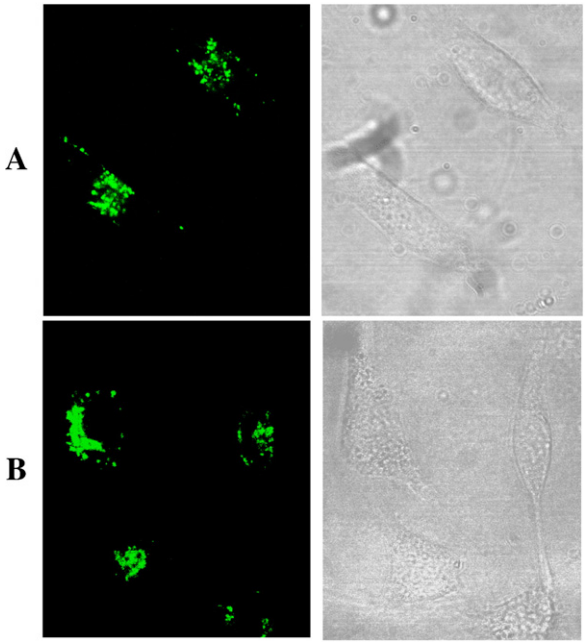

Fig. 2. Sj.GST26 uptake and localisation is independent of fluorophore and cargo. L-929 cells were incubated for 1 h with 200 nM Sj.GST26-OG (A) or 2 μM Sj.GST26-cyc3GFP (B), washed and then observed by confocal microscopy. In both cases fluorescence is in a punctate pattern in the cytoplasm. Different concentrations of the two proteins were applied because the cycle3 GFP is a less effective fluorophore than Oregon Green.

2.6. Sj.GST26 saturation

The effect of increasing concentrations of Sj.GST26-OG on L-929 cells was investigated using a FLUOstar OPTIMA fluorescent microplate reader (BMG). L-929 cells were seeded into 96-well plates (Nunclon) at a density of 1×10^4 cells per well in 10% FBS/RPMI 1640 medium and incubated overnight. The next day cells were incubated for 2 h with 0.1–20 μM Sj.GST26-OG in serum-free RPMI. Cells were then washed several times with PBS, and sample fluorescence measured in 10% FBS/PBS using a 485P excitation wavelength filter and a 520P emission wavelength filter. The kinetics of cell samples treated with trypsin to remove extracellular Sj.GST26-OG were also examined and followed the same trend, although at a lower relative fluorescence level. The viability of treated cells was assayed by means of plasma membrane integrity with Neutral Red and cellular ATP levels.

2.7. Uptake in different cell types

Subconfluent cultures of the following cell lines were treated with 200 nM Sj.GST26-OG for 2 h in serum-free medium, then harvested and prepared for flow cytometry as described above. NIH/3T3 mouse embryo fibroblast; HepG2 human hepatocyte carcinoma; Hek-293 human kidney; EL4 mouse T lymphocyte lymphoma; Jurkat human T lymphocyte leukemia; HeLa human cervical carcinoma; CV-1 African Green monkey kidney; NIT-1 mouse pancreatic beta cell insulinoma; PK(15) pig kidney; CHO-K1 Chinese hamster ovary; BT-20 human breast carcinoma; T-47D human breast duct carcinoma; JAWSII mouse myeloid immature dendritic cells; K-562 human multipotent malignant hematopoietic cells; LF2 female mouse embryonic stem cells.

Primary splenocytes were harvested from spleens of Balb/c and C57BL/6 mice by red blood cell lysis and disassociation into single cell suspension. Splenocytes were then incubated with 200 nM Sj.GST26-OG for 2 h and prepared for flow cytometry as described above.

2.8. Confocal laser scanning microscopy

Cells were seeded onto glass coverslips (Lomb Scientific) or Lab-Tek II coverglass chambers (Nunc, In Vitro Technologies) in 10% FBS/

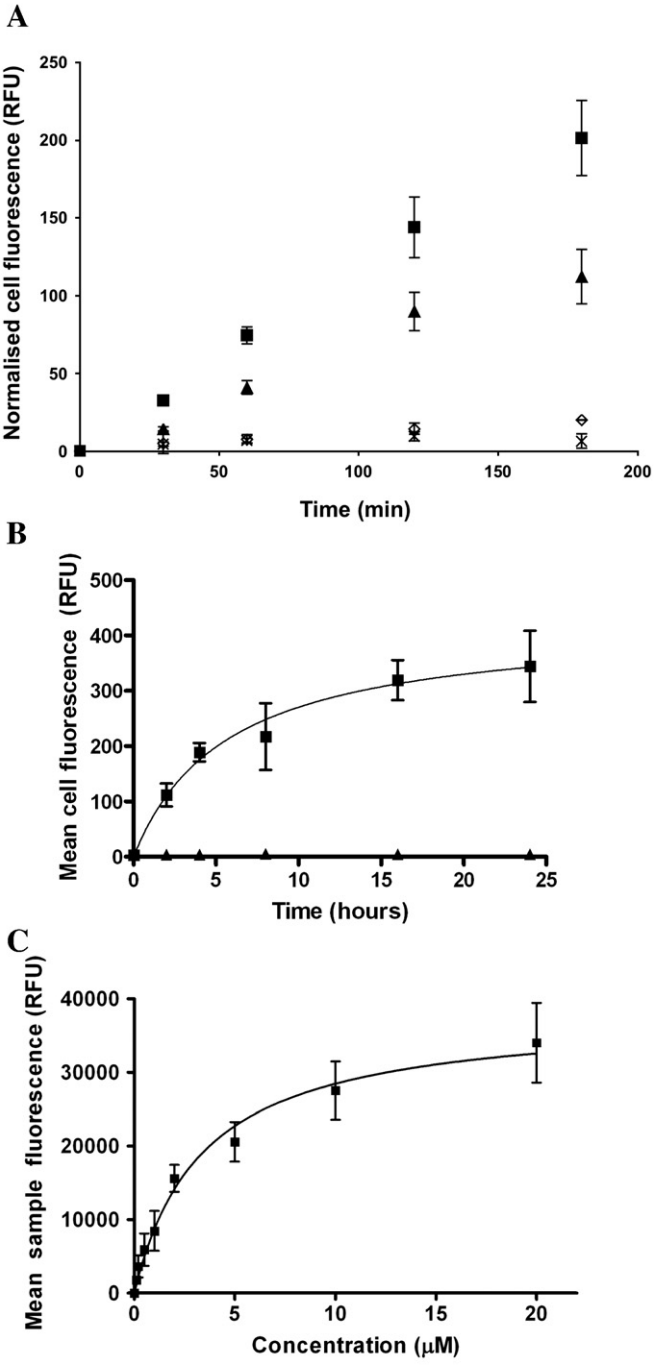

Fig. 3. Kinetics of extracellular Sj.GST26 internalisation. (A) L-929 cells were incubated with 200 nM Oregon Green-labelled Sj.GST26 (■), Tfn (▲), BSA (X) or GSH-S (◊) for the indicated time periods and intracellular fluorescence measured by flow cytometry. The mean cell fluorescence of each sample was normalised for the degree of fluorescent labelling of that protein. (B) Mean intracellular fluorescence of L-929 cells treated with Sj.GST26-OG (■) over a 24 h time period and measured by flow cytometry. Lack of 7-AAD (▲) permeability demonstrates cell viability. (C) Sample fluorescence of L-929 cells treated for 2 h with increasing concentrations of Sj.GST26-OG, as assessed by fluorescence spectroscopy. Data in all graphs is the average of three independent experiments ± SEM. (B) and (C) include a non-linear fit using the one-site binding hyperbola. Fluorescence values have been expressed as relative fluorescence units (RFU).

RPMI 1640 medium the day before experimentation. Live L-929 cells were used in microscopy experiments to avoid the possibility of artificial localisation, unless stated otherwise. All incubations were performed in serum-free RPMI 1640 medium.

Sj.GST26-OG and Sj.GST26-cyc3GFP were incubated with cells for 1 h at 200 nM and 2 μM respectively. Sj.GST26-mOrange-OG was incubated with cells at 100 nM for 2 h before addition of 400 nM bafilomycin A1 for 30 min or continued incubation of control.

To investigate endocytosis pathways, cells were serum-starved for 30 min then co-incubated with 100 nM Sj.GST26-OG plus either 0.5 mg/mL neutral dextran-TexasRed (70 kDa) or 250 nM transferrin-TRITC for 60 min.

To visualise the Golgi apparatus, cells were incubated with 5 μM BODIPY TR C_5-ceramide at 4 °C for 30 min, rinsed, then incubated with 200 nM Sj.GST26-OG at 37 °C for 1 h in fresh medium. Sj.GST26 transport in golgi-disrupted cells was investigated by pretreatment with 20 μM Brefeldin A followed by 200 nM Sj.GST26-OG incubation for 1 h. To visualise the ER, cells were first incubated with 200 nM Sj.GST26-OG for 2 h at 37 °C followed by addition of 500 nM ER-Tracker™Red for a further 15 min, then rinsed and incubated in fresh medium for 10 min. Nuclei were visualised following a 1 h treatment with 100 nM Sj.GST26-OG by fixation in 1% paraformaldehyde (15 min, room temperature), and staining with 0.5 μg/ml 7-AAD for 20 min. No change to the morphology of Sj.GST26 fluorescence was observed after fixation.

Following treatment cells were washed several times in PBS then viewed immediately in pre-warmed RPMI (in the case of coverslips within a 37 °C solution chamber). Confocal images were obtained with 60× 1.4 N.A. or 100× 1.4 N.A. oil immersion lenses of a Nikon Eclipse TE300 microscope equipped with a Biorad Radiance 2000 Laser Scanning system. Excitation was with argon and green helium neon lasers (sequentially) using 515/30 bp and E570LP emission filters. Data was recorded and analysed using LaserSharp2000 software.

3. Results

3.1. Kinetics of Sj.GST26 internalisation

Sj.GST26 has previously been shown to enter into cultured cells through qualitative microscopy methods [2]. In order to quantitatively assess the level and efficiency of cellular uptake, flow cytometry was employed to measure the intracellular accumulation of Oregon Green-labelled proteins over time. Firstly though, to eliminate any involvement from the Oregon Green fluorophore in Sj.GST26 internalisation,

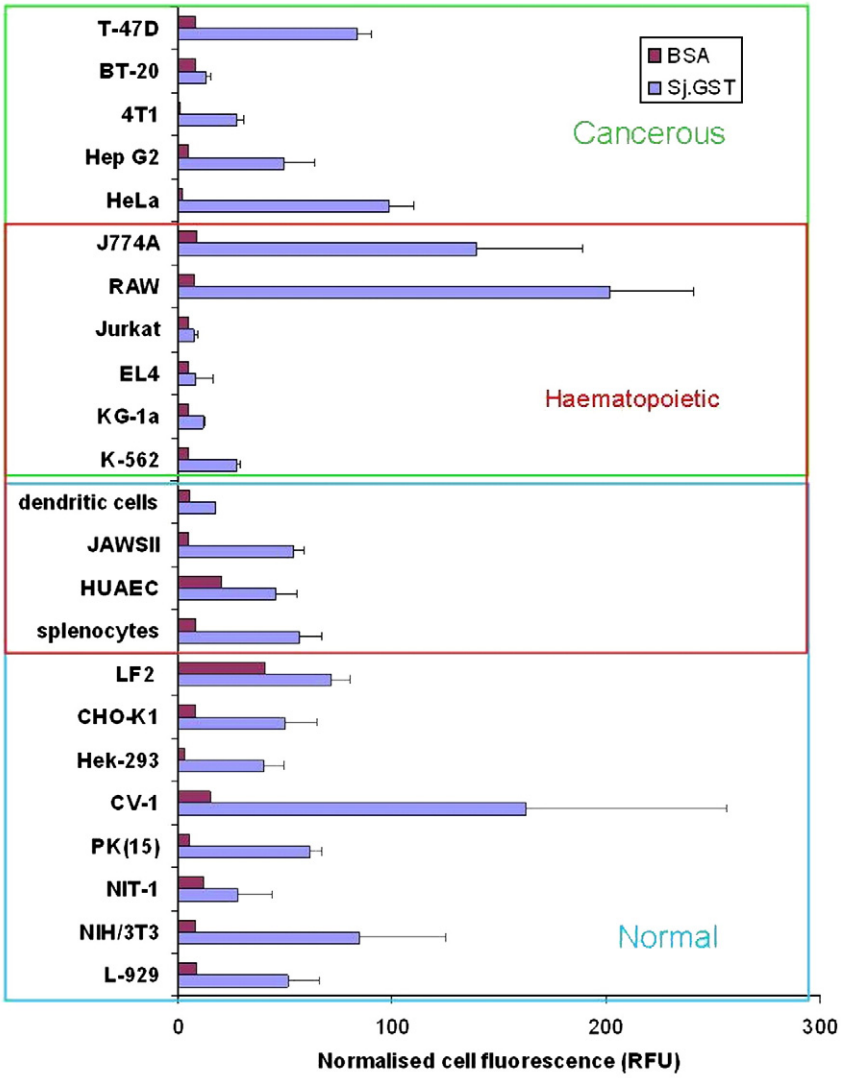

Fig. 4. Transduction of Sj.GST26 and BSA into various cell lines and primary cells. Cells were treated for 2 h with 200 nM Oregon Green-labelled Sj.GST26 or BSA then prepared for flow cytometry as per standard procedure. The mean intracellular fluorescence of each sample was normalised for the degree of fluorescent labelling of that protein. Data for Sj.GST26 is the average of duplicate measurements in two to four independent experiments + S.D., and for BSA is the average of duplicate measurements in a single experiment.

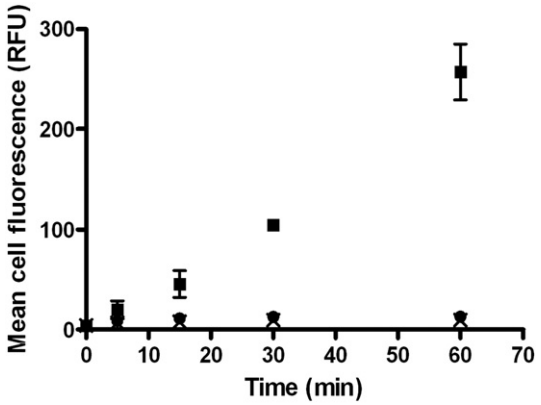

Fig. 5. Sj.GST26 internalisation is energy-dependent. L-929 cells were treated for up to 1 h with Sj.GST26-OG at low temperature (●), and in the presence (X) or absence (■) of metabolic inhibitors at 37 °C. The mean intracellular fluorescence was measured by flow cytometry. To deplete cellular ATP levels, cells were treated with 0.1% sodium azide and 50 mM 2-deoxy-D-glucose for 1 h prior to the first addition of Sj.GST26-OG. Inhibitors were maintained in the medium for the duration of Sj.GST26 treatments. After treatment with metabolic inhibitors, cellular ATP levels were measured and found to be ~25% of untreated control levels using Sigma's Bioluminescent Somatic Cell Assay kit with luminescence recorded in a 96-well plate on a Reporter Microplate 9600-001 Luminometer (Turner Biosystems). Error bars represent the S.D. of three independent experiments.

confocal microscopy was performed on live L-929 cells treated for 2 h with both Oregon Green-labelled Sj.GST26 and a Sj.GST26-cyc3GFP fluorescent fusion protein. Both the Oregon Green and GFP fluorescence appeared in a punctate pattern throughout the cytoplasm of cells (Fig. 2), confirming that Sj.GST26 is capable of membrane transduction independently of the fluorophore employed.

Flow cytometry cannot distinguish between surface-bound and internalised fluorescence so each cell sample was treated with trypsin to remove surface-bound proteins. Viable cells were then selected for analysis of intracellular Oregon Green levels through their exclusion of the membrane-impermeable 7-amino-actinomycin (7-AAD). Finally, to compare the intracellular fluorescence of different GST proteins, mean cell fluorescence values were corrected for differing levels of protein fluorescent-labelling. In this manner, intracellular accumulation of different proteins over time can be graphically represented for comparison of transduction efficiency.

A comparison of the rate of Sj.GST26 transduction into L-929 cells over 2 h, to that of human transferrin, bovine serum albumin (BSA) and human glutathione synthetase (GSH-S), is shown in Fig. 3A. Transferrin is known to be transported into cells via clathrin-mediated endocyosis and is commonly employed to probe the mechanism and efficiency of cell entry of other molecules. BSA and GSH-S were chosen as control proteins because of the comparable size of BSA to the Sj.GST26 dimer, and because like GSTs, GSH-S represents a glutathione associated enzyme. The rapidity of Sj.GST26 and transferrin internalisation above both control proteins suggests that a specific and efficient cellular mechanism is responsible for GST transduction. The same kinetic transduction profile was also produced in HeLa, 4T1 and Hek-293 cell lines (data not shown). The mouse fibroblast L-929 cell line was chosen for further mechanistic profiling of Sj.GST26 internalisation due to their normal, non-cancerous morphology. In addition, the uniform monolayer adherence and bipolar morphology of L-929 cells lends itself to clear visualisation by microscopy.

Further analysis of cells incubated with Sj.GST26 (Fig. 3B) revealed that transduction into viable cells continues for several hours before reaching equilibrium. To determine if the uptake of Sj.GST26 is related to concentration, L-929 cells were exposed to increasing concentrations of Sj.GST26 and examined by fluorescence spectroscopy after 2 h. As can be seen in Fig. 3C, the accumulation of Sj.GST26 in cells reached a plateau at concentrations above 10 μM. Even at high concentrations, Sj.GST26 does not affect cell viability (data not shown — see Methods).

3.2. Internalisation of Sj.GST26 into different cell types

The ability of Sj.GST26 to translocate into a variety of cell lines and primary tissue was assessed by flow cytometry along with BSA. As shown in Fig. 4, the capacity of different cell lines to specifically internalise Sj.GST26 is variable and with no obvious relationship to tissue type or disease status. For instance Sj.GST26 was able to translocate into multipotent myeloid cells (K-562), mouse embryonic stem cells (LF2) and primary splenocytes, but not T lymphocytes (EL4 and Jurkat), as judged by comparison of normalised Sj.GST26 and BSA intracellular fluorescence. Also, transduction into two breast carcinoma lines (BT-20 and T-47D) differed widely. Although no trend for Sj.GST26 internalisation is apparent from Fig. 4, this study clearly shows that the accumulation of Sj.GST26 by cells is not an uncommon occurrence.

3.3. Mechanism of Sj.GST26 transduction

Given that the punctate pattern of Sj.GST26 fluorescence in cells is reminiscent of endosomes in the cytoplasm, we assessed the involvement of endocytosis in Sj.GST26 accumulation. The ability of cells to internalise Sj.GST26 at 4 °C and the role of ATP in transduction were examined using flow cytometry. As demonstrated in Fig. 5, low temperature and cellular ATP depletion precluded cellular uptake of Sj.GST26, indicating that Sj.GST26 internalisation is an energy-dependent process. To probe the nature of the intracellular environment of Sj.GST26, a Sj.GST26 fusion protein containing the pH-sensitive fluorescent mOrange protein (pK_a 6.5) was created. Subsequent Oregon Green-labelling (pK_a 4.7) of this

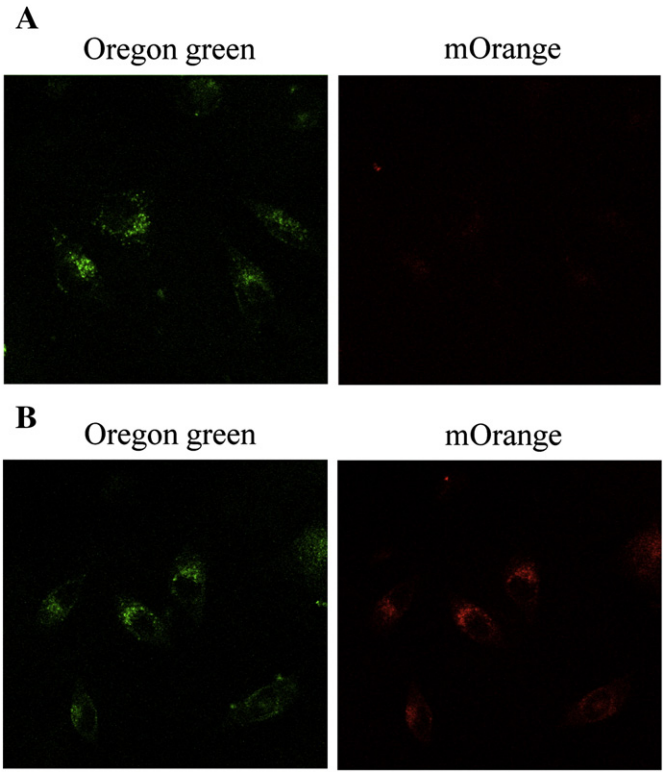

Fig. 6. Sj.GST26 localises to acidic vesicles. Sj.GST26 localises to acidic vesicles. L-929 cells were treated with 100 nM Sj.GST26-mOrange-OG for 21/2 h (A) or 2 h plus 30 min with 400 nM bafilomycin A1 to prevent endosome acidification (B). Both samples were washed and observed by confocal microscopy using the same laser settings for both samples.

molecule enabled two-colour confocal microscopy, where the two fluorophores were differentially sensitive to pH changes. After 2 h incubation with the Sj.GST26-mOrange-OG molecule, strong green fluorescence could be visualised but only a faint orange signal. When bafilomycin A1, a selective inhibitor of vacuolar H^+-ATPases [17], was subsequently added to cells however, a considerable increase in the level of orange fluorescence was seen (Fig. 6). This novel experiment confirms that Sj.GST26 accumulates in acidic vesicles within cells. Control cells incubated with the mOrange protein alone displayed no fluorescence, verifying that the Sj.GST26 portion of the fusion protein is responsible for its cellular transport (data not shown).

3.4. Intracellular fate of Sj.GST26

The mechanism of endocytosis employed by a molecule plays a critical role in determining its fate, both in terms of its destination and stability. The nature of the Sj.GST26 endocytic route was probed using traditional endocytosis 'markers' in confocal microscopy experiments. These markers included transferrin for clathrin-mediated endocytosis (CME) [18] and neutral dextran for macropinocytosis [19–21]. As illustrated in Fig. 7, Sj.GST26 clearly colocalised with vesicles containing both fluorescent markers. Since dextran is a fluid-phase marker it potentially has access not only to macropinosomes, but any endocytic vesicle formed within cells provided they are large enough to encapsulate the molecule [22]. It is therefore possible that this marker does not exclusively represent macropinosomes. It must also be noted that colocalisation with transferrin does not necessarily indicate CME. Experiments using chlorpromazine and K^+ depletion (which are both known to affect CME) show that uptake is substantially reduced (see Supplementary material).

To begin to understand the physiological functionality behind GST transduction, we sought to further clarify the subcellular localisation of exogenous Sj.GST26. Through confocal microscopy we have observed that Sj.GST26 is localised to endosomes within minutes of cellular incubation (data not shown). Subsequent fixation and nuclear staining of cells loaded with Sj.GST26 (Fig. 8A) revealed that these vesicles accumulate in a discrete perinuclear region after 1 h. The Golgi apparatus, also located adjacent to the nucleus, is pivotal to membrane traffic affecting transport within both endocytic and secretory pathways [23]. We examined whether Sj.GST26-containing vesicles migrate to a region of cells stained with BODIPY TR C_5-ceramide, a structural marker for the Golgi complex [24]. Fig. 8B shows that vesicular Sj.GST26 fluorescence, whilst predominantly situated in regions stained with C_5-ceramide, is not sufficiently colocalised to indicate that these vesicles are docking with the Golgi apparatus. For comparison, an endoplasmic reticulum labelling drug, ER-Tracker™ Red, was employed and also found distributed within a perinuclear region similar to both the Golgi marker and Sj.GST26 localised areas of L-929 cells (Fig. 8C). Given these results, it is difficult to conclude whether Sj.GST26-containing vesicles are migrating to the Golgi complex. However confocal microscopy of cells treated with brefeldin A, which disrupts traffic within the *trans*-Golgi network [25,26], did not change the perinuclear localisation of Sj.GST26 vesicles (data not shown) inferring that vesicles are not interacting with the Golgi complex.

Clathrin-coated pits containing transferrin are sorted for recycling in a perinuclear region of the cell termed the perinuclear recycling compartment (PNRC) [22,27], which has a pH ~5.6 and is physically distinct from the Golgi apparatus [28]. Dextran-filled late endosomes and lysosomes also accumulate in a perinuclear region separate to the Golgi which is proposed to be the PNRC [28]. Given the potential involvement of CME and macropinocytosis in Sj.GST26 transduction, and the absence of colocalisation with the Golgi apparatus, it seems likely that fluorescent Sj.GST26 accumulates in the PNRC for further processing. Whether Sj.GST26 is subsequently degraded, recycled to

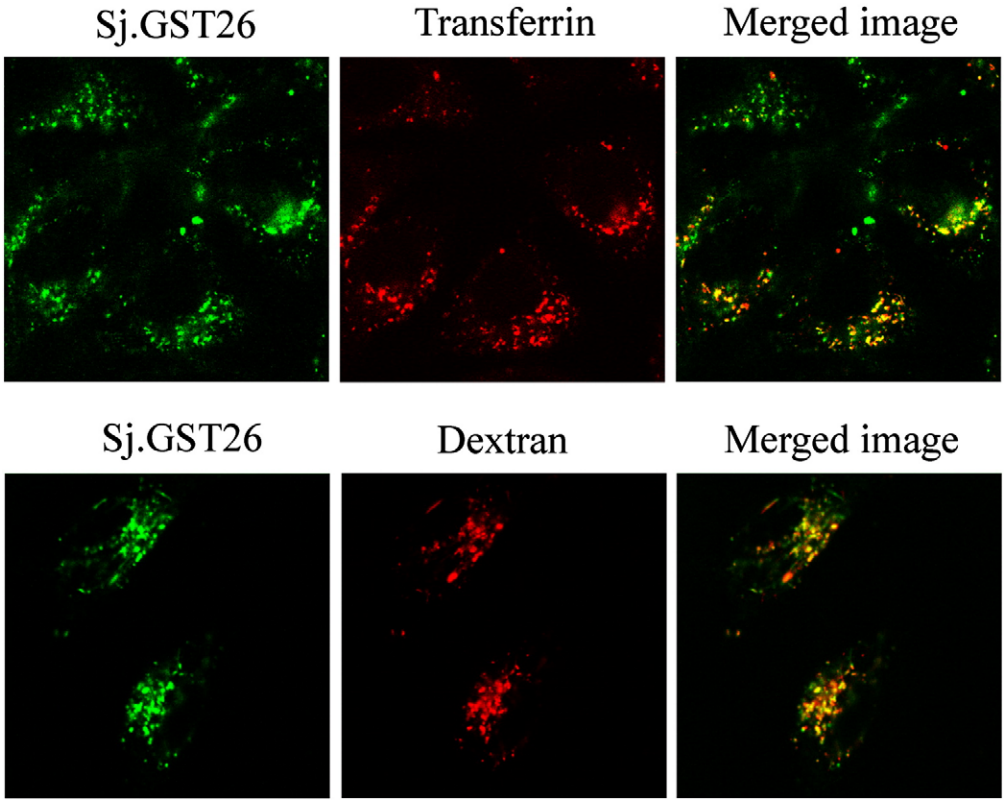

Fig. 7. Colocalisation between Sj.GST26 and different endocytic pathway markers. L-929 cells were serum-starved for 30 min then co-incubated with 100 nM Sj.GST26-OG plus either 250 nM transferrin-TRITC (upper panel) or 0.5 mg/mL dextran-TexasRed (lower panel) for 60 min. Cells were washed and observed live by confocal microscopy. Note the significant colocalisation (yellow) between Sj.GST26 and both transferrin and neutral dextran.

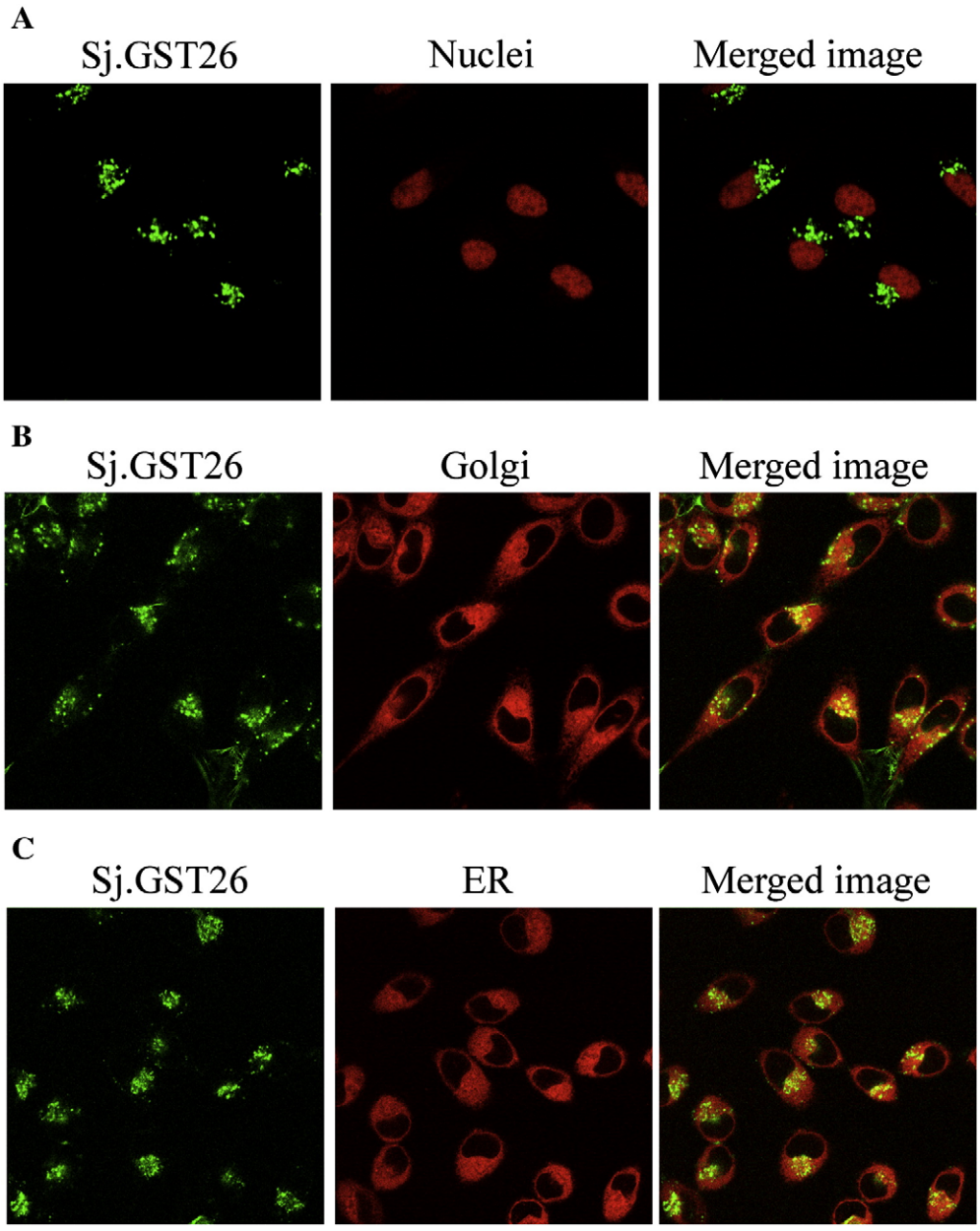

Fig. 8. Perinuclear Sj.GST26 fluorescence is not localised to the Golgi or ER. (A) L-929 cells treated for 1 h with Sj.GST26-OG were fixed and nuclei stained with 7-AAD. Note the perinuclear punctate fluorescence of Sj.GST26. To investigate this region of Sj.GST26 fluorescence, L-929 cells were stained with BODIPY TR C_5-ceramide for 30 min at 4 °C for Golgi visualisation, washed, then incubated with Sj.GST26-OG for 1 h (B), or incubated with Sj.GST26-OG for 2 h then ER-Tracker™ Red added for a further 15 min to visualise the endoplasmic reticulum (C). Whilst Sj.GST26 fluorescence is within the region of both the Golgi and ER, pixels in merged images do not overlap thereby ruling out colocalisation.

the extracellular matrix or released to the cytoplasm in small quantities (as suggested in [2]), is yet to be clarified, but preliminary results demonstrate that intracellular Oregon Green fluorescence is stable for several hours.

3.5. The GST-fold motif determines cell transduction

The cytosolic GST gene family can be subdivided into a number of different classes which, despite having relatively low sequence homology, share a similar structure known as the 'GST-fold' (Fig. 1) [11]. In addition to these classical GSTs, four proteins that contain the GST-fold but possess no significant glutathione-conjugating enzyme activity have been identified — human CLIC2 (Chloride Intracellular Channel 2) and GDAP1 (Ganglioside-induced differentiation-associated protein 1), *S. cerevisiae* Ure2 and *E. coli* Glutaredoxin-2 (Grx2). The functions of these 'GST-fold' proteins vary widely; CLIC2 acts to regulate the cardiac ryanodine receptor 2 channels [12,29,30], GDAP1 is highly expressed in the whole brain and spinal cord with mutations causing damage to the peripheral nervous system (Charcot-Marie-Tooth disease) [14], Ure2 acts to negatively regulate GATA factor-mediated transcription in yeast [31], and Grx2 catalyses GSH-disulfide oxidoreductions [32].

To determine if the GST-fold structure is important for membrane transduction, we examined the ability of several mammalian cytosolic GST isoforms and the four non-GST proteins possessing a GST-fold, to penetrate L-929 cells along with Sj.GST26. The cellular uptake of all proteins was quantitatively evaluated over time by flow cytometry analysis (see Methods), and the standardised intracellular fluorescence after 3 h incubation is displayed in Fig. 9. The most efficient transduction was produced by the protein CLIC2, and all other GST and GST-fold proteins fall in a tight range above the two negative control proteins, BSA and GSH-S. In light of these results, key amino acids that

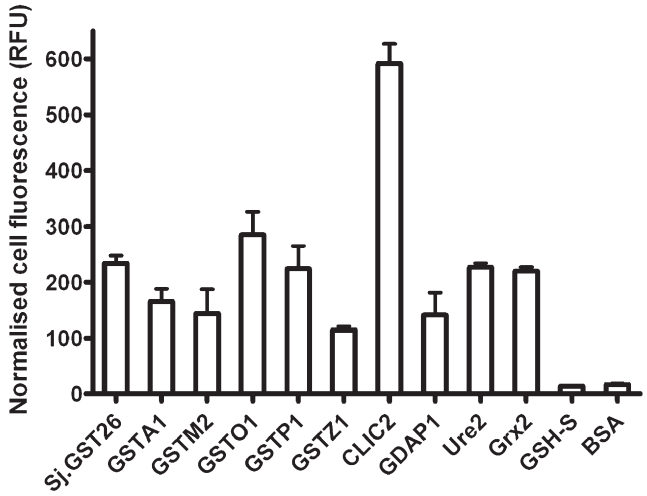

Fig. 9. Proteins containing a GST-fold structure are efficiently internalised by L-929 cells. Cells were incubated with 200 nM Oregon Green-labelled proteins for 3 h and intracellular fluorescence measured by flow cytometry. The mean cell fluorescence of each sample was normalised for the degree of fluorescent labelling of that protein. Error bars represent the SEM of three independent experiments.

are known to be critical in GST enzyme activity were also examined for their role in transduction. Intriguingly, the cellular uptake of the GSTA1, GSTM2 and GSTO1 mutants (Y9F, Y7F and C32A respectively), exceeded that of the wild-type proteins by 1.4 to 5-fold (Fig. 10). The fact that wild-type GST enzymes, their active-site mutants, and the GST-fold proteins are all capable of efficient internalisation into L-929 cells, suggests that it is the structural fold of these proteins that enables membrane transduction. The route of uptake of GSTs from the Zeta and Mu classes was further characterised in the presence of several metabolic inhibitors and endocytosis markers, and found to share the same trends of inhibition and colocalisation profiles as Sj. GST26 (data not shown), indicating that the same endocytosis pathways are utilised in the uptake of these GST-fold proteins.

4. Discussion

In this study we examined the internalisation kinetics, cellular specificity and mechanism of cellular entry of a GST from *S. japonicum* using quantitative flow cytometry and confocal microscopy. In addition, a quantitative comparison of the transduction efficiency of a range of mammalian GSTs from different evolutionary classes, as well as proteins with a GST-fold structure but lacking GST enzyme activity, was undertaken.

Comparative analysis of the cellular uptake of fluorescently-labelled Sj.GST26, transferrin, BSA and GSH-S demonstrated that the rate of cellular Sj.GST26 uptake is more rapid than transferrin, whilst the internalisation of control proteins BSA and GSH-S is minimal. This suggests that the mechanism underlying Sj.GST26 transduction is a rapid and efficient process and not simply a background event resulting from constitutive sampling of the culture medium. Visualisation of Sj.GST26 in cells revealed punctate cytoplasmic fluorescence, and the pH sensitive fusion protein Sj.GST26-mOrange further demonstrated that these punctate vesicles are acidic in nature, implicating endocytosis as the process responsible for internalisation. These microscopy studies were performed on live cells to avoid any possibility of artificial distribution from fixation, however the morphology of punctate vesicles did not alter when cells were fixed to allow nuclei labelling. In addition, the intracellular fluorescence of Sj.GST26-GFP eliminated any involvement of the Oregon Green fluorophore in Sj.GST26 transduction for this and previous studies [2].

A role for endocytosis in Sj.GST26 uptake was further supported by the prevention of intracellular Sj.GST26 fluorescence after cellular energy depletion, and colocalisation of internalised protein with transferrin and dextran marker molecules. These results are in keeping with recent data providing evidence for endocytic mechanisms in the cell entry of many protein transduction domains [33–37]. Endocytosis is responsible for the internalisation of hormones, growth factors, plasma proteins and recycling of membrane components and receptors and can occur through several distinct pathways within cells, including macropinocytosis, CME, caveolin-mediated, and clathrin- and caveolin-independent lipid raft pathways (reviewed in [38]).

The mechanism of uptake of an endocytosed molecule is known to influence its subsequent intracellular trafficking and fate, which is of major significance to the delivery of therapeutics into cells. The migration of Sj.GST26-containing vesicles to a region consistent with the perinuclear recycling compartment of cells is in agreement with the employment of either CME or macropinocytosis pathways in Sj. GST26 transduction, as late endosomes, lysosomes and recycling endosomes are all known to accumulate in this subcellular compartment [22,27,28]. It must be noted however, that the interconnecting networks of endocytosis are poorly delineated, and macropinocytosis markers (as well as lipid raft markers) have been demonstrated to penetrate cells through multiple routes and also merge at the stage of early endosomes [28,39,40]. It is therefore not possible to specify the intracellular fate of this class of proteins after internalisation.

The cytosolic GST gene family can be subdivided into a number of different classes that may be represented in a related group of species or be found over a wide phylogenetic range [11]. Usually, the sequence identity between classes is less than 30% and is around 60% or higher within classes [41]. In mammals, seven classes of cytosolic GST have been described (Alpha, Mu, Omega, Pi, Sigma, Theta and Zeta) and there may be multiple genes within each class [42]. Given that Sj. GST26 has proven to be an efficient cell transduction protein, we wished to assess the ability of proteins from the mammalian cytosolic GST classes to penetrate cells alongside Sj.GST26. Despite sharing little primary sequence identity and utilising different active-site residues, all cytosolic GST classes have the same basic structural fold. This GST-fold consists of an N-terminal thioredoxin fold followed by a strongly helical C-terminal domain [11], and is also possessed by a range of 'GST-fold' proteins which have no glutathione-dependent enzyme activity. We therefore quantitatively compared the transduction efficiency of GST proteins in parallel with several GST-fold proteins. GSH-S was also included in this comparative study as a structural

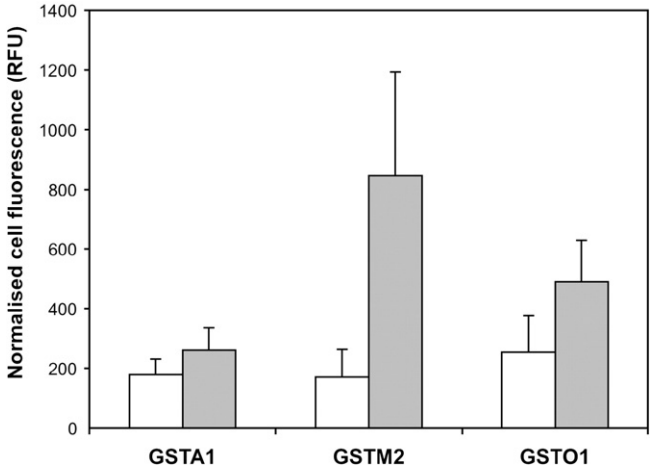

Fig. 10. Active-site mutants of GSTs show increased cellular uptake in L-929 cells compared with wild-type GSTs. The effect of mutating catalytically important residues on GST transduction was examined for GSTA1 (Y9F), GSTM2-2 (Y7F) and GSTO1 (C32A). L-929 cells were incubated with 200 nM Oregon Green-labelled proteins for 3 h and intracellular fluorescence measured by flow cytometry. The mean cell fluorescence of each sample was normalised for the degree of fluorescent labelling of that protein. Error bars represent the S.D. of three independent experiments.

negative control since it has the ability to bind glutathione, but does not share the GST-fold conformation.

All classes of GST tested so far have proven capable of rapid cell transduction. In addition the four GST-fold proteins were also internalised, in fact one of these proteins, CLIC2, was the most efficiently transported. This indicates that the GST-fold structure is a common feature present in cellular transduction and the enzymic property of GST is not related to its ability to enter cells. Further evidence for this hypothesis lies with the mutation of catalytically important GST residues which, rather than impeding cell transduction capacity, show a propensity to elevate the efficiency of cell entry. Curiously, it has previously been shown that CLIC proteins, as well as being members of the cytosolic GST structural family, can modulate ryanodine receptor Ca^{2+} channels [43] and under certain conditions even undergo a conformational change to enter membranes and form ion channels directly [44]. It is possible that other GSTs may also enter cell membranes to a limited extent, and this may facilitate or even stimulate endocytosis. This concept is supported by the observation that endogenous alpha class GSTs are capable of being reversibly incorporated into, or in close proximity with, the plasma and nuclear membranes of cells [4,5].

It has long been known that upon liver damage or disease there is a large release of GSTs into the blood circulation. However, the half-life of this circulating GST population is surprisingly short which previously has been assumed to be due to degradation [45]. It is an enticing notion to consider that rather than degradation, the loss of circulating GST may be due to an inherent transduction mechanism that allows external GST to be transported back into neighbouring cells, with the potential to enhance self-defense in these cells to toxins or free radicals that caused their initial release.

The mechanistic profile of Sj.GST26 transduction outlined in this study provides quantitative information on the efficiency and manner in which GST-fold proteins may enter cells. We have shown that this transport occurs through an energy-dependent process involving endocytosis that also demonstrates cell specificity. Moreover, we establish that proteins adopting a GST-fold are capable of traversing into cells, and may represent a new class of transduction molecule.

Acknowledgements

This work was supported by grant DP0558315 from the Australian Research Council.

Appendix A. Supplementary data

Supplementary data associated with this article can be found, in the online version, at doi:10.1016/j.bbamem.2008.10.018.

References

[1] P. Watson, R.A. Spooner, Toxin entry and trafficking in mammalian cells, Adv. Drug Deliv. Rev. 58 (2006) 1581–1596.
[2] S. Namiki, T. Tomida, M. Tanabe, M. Iino, K. Hirose, Intracellular delivery of glutathione S-transferase into mammalian cells, Biochem. Biophys. Res. Commun. 305 (2003) 592–597.
[3] H. Murata, J. Futami, M. Kitazoe, T. Yonehara, H. Nakanishi, M. Kosaka, H. Tada, M. Sakaguchi, Y. Yagi, M. Seno, N.H. Huh, H. Yamada, Intracellular delivery of glutathione S-transferase-fused proteins into mammalian cells by polyethylenimine-glutathione conjugates, J. Biochem. 144 (2008) 447–455.
[4] L. Stella, V. Pallottini, S. Moreno, S. Leoni, F. De Maria, P. Turella, G. Federici, R. Fabrini, K.F. Dawood, M.L. Bello, J.Z. Pedersen, G. Ricci, Electrostatic association of glutathione transferase to the nuclear membrane. Evidence of an enzyme defense barrier at the nuclear envelope, J. Biol. Chem. 282 (2007) 6372–6379.
[5] N. Merezhinskaya, G.A. Kuijpers, Y. Raviv, Reversible penetration of alpha-glutathione S-transferase into biological membranes revealed by photosensitized labelling in situ, Biochem. J. 335 (1998) 597–604.
[6] R.T. Baker, S.A. Smith, R. Marano, J. McKee, P.G. Board, Protein expression using cotranslational fusion and cleavage of ubiquitin. Mutagenesis of the glutathione-binding site of human Pi class glutathione S-transferase, J. Biol. Chem. 269 (1994) 25381–25386.
[7] P.G. Board, K. Pierce, Expression of human glutathione S-transferase 2 in *Escherichia coli*. Immunological comparison with the basic glutathione S-transferases isoenzymes from human liver, Biochem. J. 248 (1987) 937–941.
[8] V.L. Ross, P.G. Board, Molecular cloning and heterologous expression of an alternatively spliced human Mu class glutathione S-transferase transcript, Biochem. J. 294 (1993) 373–380.
[9] D.B. Smith, K.S. Johnson, Single-step purification of polypeptides expressed in *Escherichia coli* as fusions with glutathione S-transferase, Gene 67 (1988) 31–40.
[10] A.C. Blackburn, H.F. Tzeng, M.W. Anders, P.G. Board, Discovery of a functional polymorphism in human glutathione transferase zeta by expressed sequence tag database analysis, Pharmacogenetics 10 (2000) 49–57.
[11] P.G. Board, M. Coggan, G. Chelvanayagam, S. Easteal, L.S. Jermiin, G.K. Schulte, D.E. Danley, L.R. Hoth, M.C. Griffor, A.V. Kamath, M.H. Rosner, B.A. Chrunyk, D.E. Perregaux, C.A. Gabel, K.F. Geoghegan, J. Pandit, Identification, characterization, and crystal structure of the Omega class glutathione transferases, J. Biol. Chem. 275 (2000) 24798–24806.
[12] P.G. Board, M. Coggan, S. Watson, P.W. Gage, A.F. Dulhunty, CLIC-2 modulates cardiac ryanodine receptor Ca2+ release channels, Int. J. Biochem. Cell. Biol. 36 (2004) 1599–1612.
[13] R.R. Gali, P.G. Board, Sequencing and expression of a cDNA for human glutathione synthetase, Biochem. J. 310 (1995) 353–358.
[14] A.J. Shield, T.P. Murray, P.G. Board, Functional characterisation of ganglioside-induced differentiation-associated protein 1 as a glutathione transferase, Biochem. Biophys. Res. Commun. 347 (2006) 859–866.
[15] A.M. Catanzariti, T.A. Soboleva, D.A. Jans, P.G. Board, R.T. Baker, An efficient system for high-level expression and easy purification of authentic recombinant proteins, Protein. Sci. 13 (2004) 1331–1339.
[16] N.C. Shaner, R.E. Campbell, P.A. Steinbach, B.N. Giepmans, A.E. Palmer, R.Y. Tsien, Improved monomeric red, orange and yellow fluorescent proteins derived from *Discosoma* sp. red fluorescent protein, Nat. Biotechnol. 22 (2004) 1567–1572.
[17] M.J. Clague, S. Urbe, F. Aniento, J. Gruenberg, Vacuolar ATPase activity is required for endosomal carrier vesicle formation, J. Biol. Chem. 269 (1994) 21–24.
[18] A. Benmerah, V. Poupon, N. Cerf-Bensussan, A. Dautry-Varsat, Mapping of Eps15 domains involved in its targeting to clathrin-coated pits, J. Biol. Chem. 275 (2000) 3288–3295.
[19] U.S. Huth, R. Schubert, R. Peschka-Suss, Investigating the uptake and intracellular fate of pH-sensitive liposomes by flow cytometry and spectral bio-imaging, J. Control. Release 110 (2006) 490.
[20] H.L. Amand, K. Fant, B. Norden, E.K. Esbjorner, Stimulated endocytosis in penetratin uptake: effect of arginine and lysine, Biochem. Biophys. Res. Commun. 371 (2008) 621–625.
[21] A.T. Jones, Macropinocytosis: searching for an endocytic identity and role in the uptake of cell penetrating peptides, J. Cell. Mol. Med. 11 (2007) 670–684.
[22] G.n. Baravalle, D. Schober, M. Huber, N. Bayer, R.F. Murphy, R. Fuchs, Transferrin recycling and dextran transport to lysosomes is differentially affected by bafilomycin, nocodazole, and low temperature, Cell Tissue Res. 320 (2005) 99.
[23] J.S. Bonifacino, R. Rojas, Retrograde transport from endosomes to the trans-Golgi network, Nat. Rev. Mol. Cell. Biol. 7 (2006) 568.
[24] R.E. Pagano, O.C. Martin, H.C. Kang, R.P. Haugland, A novel fluorescent ceramide analogue for studying membrane traffic in animal cells: accumulation at the Golgi apparatus results in altered spectral properties of the sphingolipid precursor, J. Cell Biol. 113 (1991) 1267–1279.
[25] P.A. Orlandi, P.K. Curran, P.H. Fishman, Brefeldin A blocks the response of cultured cells to cholera toxin. Implications for intracellular trafficking in toxin action, J. Biol. Chem. 268 (1993) 12010–12016.
[26] D. Drecktrah, P. de Figueiredo, R.M. Mason, W.J. Brown, Retrograde trafficking of both Golgi complex and TGN markers to the ER induced by nordihydroguaiaretic acid and cyclofenil diphenol, J. Cell. Sci. 111 (1998) 951–965.
[27] J.G. Magadan, M.A. Barbieri, R. Mesa, P.D. Stahl, L.S. Mayorga, Rab22a regulates the sorting of transferrin to recycling endosomes, Mol. Cell. Biol. 26 (2006) 2595–2614.
[28] S. Sabharanjak, P. Sharma, R.G. Parton, S. Mayor, GPI-anchored proteins are delivered to recycling endosomes via a distinct cdc42-regulated, clathrin-independent pinocytic pathway, Dev. Cell. 2 (2002) 411–423.
[29] A.F. Dulhunty, P. Pouliquin, M. Coggan, P.W. Gage, P.G. Board, A recently identified member of the glutathione transferase structural family modifies cardiac RyR2 substate activity, coupled gating and activation by Ca2+ and ATP, Biochem. J. 390 (2005) 333–343.
[30] B.A. Cromer, M.A. Gorman, G. Hansen, J.J. Adams, M. Coggan, D.R. Littler, L.J. Brown, M. Mazzanti, S.N. Breit, P.M. Curmi, A.F. Dulhunty, P.G. Board, M.W. Parker, Structure of the Janus protein human CLIC2, J. Mol. Biol. 374 (2007) 719–731.
[31] R. Rai, J.J. Tate, T.G. Cooper, Ure2, a prion precursor with homology to glutathione S-transferase, protects *Saccharomyces cerevisiae* cells from heavy metal ion and oxidant toxicity, J. Biol. Chem. 278 (2003) 12826–12833.
[32] A. Vlamis-Gardikas, A. Potamitou, R. Zarivach, A. Hochman, A. Holmgren, Characterization of *Escherichia coli* null mutants for glutaredoxin 2, J. Biol. Chem. 277 (2002) 10861–10868.
[33] G. Drin, S. Cottin, E. Blanc, A.R. Rees, J. Temsamani, Studies on the internalization mechanism of cationic cell-penetrating peptides, J. Biol. Chem. 278 (2003) 31192–31201.
[34] A. Fittipaldi, A. Ferrar, M. Zoppe, C. Arcangeli, V. Pellegrini, F. Beltram, M. Giacca, Cell membrane lipid rafts mediate caviolar endocytosis of HIV-1 Tat fusion proteins, J. Biol. Chem. 278 (2003) 34141–34149.
[35] I.A. Khalil, K. Kogure, S. Futaki, H. Harashima, High density of octaarginine stimulates macropinocytosis leading to efficient intracellular trafficking for gene expression, J. Biol. Chem. 281 (2005) 3544–3551.

[36] M. Lundberg, S. Wikstrom, M. Johansson, Cell surface adherence and endocytosis of protein transduction domains, Mol. Ther. 8 (2003) 143–150.
[37] J.S. Wadia, R.V. Stan, S.F. Dowdy, Transducible TAT-HA fusogenic peptide enhances escape of TAT-fusion proteins after lipid raft macropinocytosis, Nat. Med. 10 (2004) 310–315.
[38] S.D. Conner, S.L. Schmid, Regulated portals of entry into the cell, Nature 422 (2003) 37.
[39] M. Kirkham, R.G. Parton, Clathrin-independent endocytosis: new insights into caveolae and non-caveolar lipid raft carriers, Biochim. Biophys. Acta (BBA) — Mol. Cell Res. 1745 (2005) 273–286.
[40] M.L. Torgersen, G. Skretting, B. van Deurs, K. Sandvig, Internalization of cholera toxin by different endocytic mechanisms, J. Cell. Sci. 114 (2001) 3737–3747.
[41] J. Li, Z. Xia, J. Ding, Thioredoxin-like domain of human {kappa} class glutathione transferase reveals sequence homology and structure similarity to the {theta} class enzyme, Protein. Sci. 14 (2005) 2361–2369.
[42] B. Mannervik, P.G. Board, J.D. Hayes, I. Listowsky, W.R. Pearson, Nomenclature for mammalian soluble glutathione transferases, Methods Enzymol. 401 (2005) 1–8.
[43] A. Dulhunty, P. Gage, S. Curtis, G. Chelvanayagam, P. Board, The glutathione transferase structural family includes a nuclear chloride channel and a ryanodine receptor calcium release channel modulator, J. Biol. Chem. 276 (2001) 3319–3323.
[44] D.R. Littler, S.J. Harrop, W.D. Fairlie, L.J. Brown, G.J. Pankhurst, S. Pankhurst, M.Z. DeMaere, T.J. Campbell, A.R. Bauskin, R. Tonini, M. Mazzanti, S.N. Breit, P.M. Curmi, The intracellular chloride ion channel protein CLIC1 undergoes a redox-controlled structural transition, J. Biol. Chem. 279 (2004) 9298–9305.
[45] G.J. Beckett, E.H. Dyson, B.J. Chapman, A.J. Templeton, J.D. Hayes, Plasma glutathione S-transferase measurements by radioimmunoassay: a sensitive index of hepatocellular damage in man, Clin. Chim. Acta 146 (1985) 11–19.